3. METHODOLOGY: DEVELOPMENT OF A SLOPE FAILURE PREDICTION MODEL FOR SURFACE MINES (SFPMSM)

Predicting mine slope failures is highly challenging due to their complex nature. Understanding their behaviour is crucial for risk management, reducing damage, and ensuring safety. Slope monitoring and remote sensing tools like SSR play vital roles in identifying pre-failure signs. Researchers have explored various theories, with creep theory being a widely utilized approach for predicting acceleration phases and slope failures (Crosta & Agliardi, 2003; Saito, 1969). In particular, Fukuzono's initially presented the Inverse Velocity Method (IVM), which was used to make failure predictions in the literature (FUKUZONO, 1985b). The findings were generally positive (Rose & Hungr, 2007a). Despite extensive research, accurately predicting slope failures in mines remains a persistent challenge. Understanding and tracking slope development through datasets are crucial for forecasting. Identifying the onset of the acceleration phase is particularly critical for effectively utilizing prediction methods and assessing likely behaviours accurately (Dick et al., 2015a). The determination of the onset of acceleration (OOA) and subsequent failure forecasting has traditionally been done manually (Dick et al., 2015a; Petley, 2004; Rose & Hungr, 2007a; Voight & Kennedy, 1979). Manual methods, while extensively used, lack automation, resulting in inefficient real-time assessment for slope behaviour and failure prediction. This absence of automation hinders timely responses and emergency warnings, making them less ideal for critical situations or rapid response requirements. Nevertheless, even with all these works on landslides and various natural and artificial structures (Carlà, Intrieri, di Traglia, et al., 2017), a standard approach for determining the onset of the tertiary creep phase has not yet been established.

The hypothesis for this work is " The integration of ground-based radar data and an analysis of deformation behaviours, combined with historical slope failure patterns, using predictive modeling in a software, will allow the development of a robust predictive model for surface mine slope failures." The technical rationale supporting this hypothesis has been divided into; SSR data, deformation behaviours, historical slope failure patterns, integration of multiple data sources, and predictive modeling.

Ground-based radar, like Slope Stability Radar (SSR), provides real-time, high-resolution data on slope deformations. The hypothesis suggests that leveraging this data, encompassing displacement, velocity, and deformation patterns, enables accurate monitoring of slope behaviour and early detection of potential failures through predictive modeling. Understanding the deformation behaviour of the slope, including rates and unusual patterns, is crucial for failure prediction, acknowledging its importance in detecting early warning signs of instability. Analysing past slope failures offers insights into triggers, acceleration phases, velocity patterns, and behaviours, enriching the predictive model by learning from historical failure patterns. Integrating diverse data sources like ground-based radar, deformation behaviour, surveys, and historical records enhances the accuracy and reliability of the predictive model. Utilizing software such as MATLAB for predictive modeling facilitates efficient data processing and analysis, aiding in pattern recognition and correlation identification, thus fostering the development of an accurate predictive model for surface mine slope failures.

The proposed hypothesis aligns with leveraging modern technology (ground-based radar) and historical data to develop a predictive model. This model aims to enhance proactive slope management, improve safety protocols, and ultimately reduce the occurrence and impact of slope failures in surface mining operations.

3.1 Initial Stages of Data Analysis

While beginning our work we tried to use the already established inverse velocity method to predict slope failures in open cast mines by finding out the Threshold Limit Velocity (TLV). This section presents the work in the initial stages of the project to understand slope behaviours and find thresholds. The data used for prediction was mainly from Kusmunda Mine, SECL. To meet the above objectives of the research, field visits were conducted in June'2018 & March'2019 to assess the condition on-site, and working out the modus operandi for smooth data transfer and timely analysis of monitoring data. A number of field visits were also made to nearby Gevra and Dipka mines of SECL. Subsequently, the mine management transferred the monitoring data acquired by it in different time periods and at different locations of monitoring for necessary analysis. The SSR was placed at 100 m from the slopes that were used for the data collection and further analysis. The climate of the mining area is generally dry to moist tropical with temperature varying between 6 to 48^0 C. Figure 3.1 shows the pictorial view of the slope face considered for this purpose.

Figure 3. 1 : Image of the face/wall being monitored (June 2018)

Fig. 3.2 shows the plots of enhanced deformation and inverse velocity averaged over 60 and 1440 minutes in the selected pixel from the same wall with respect to time.

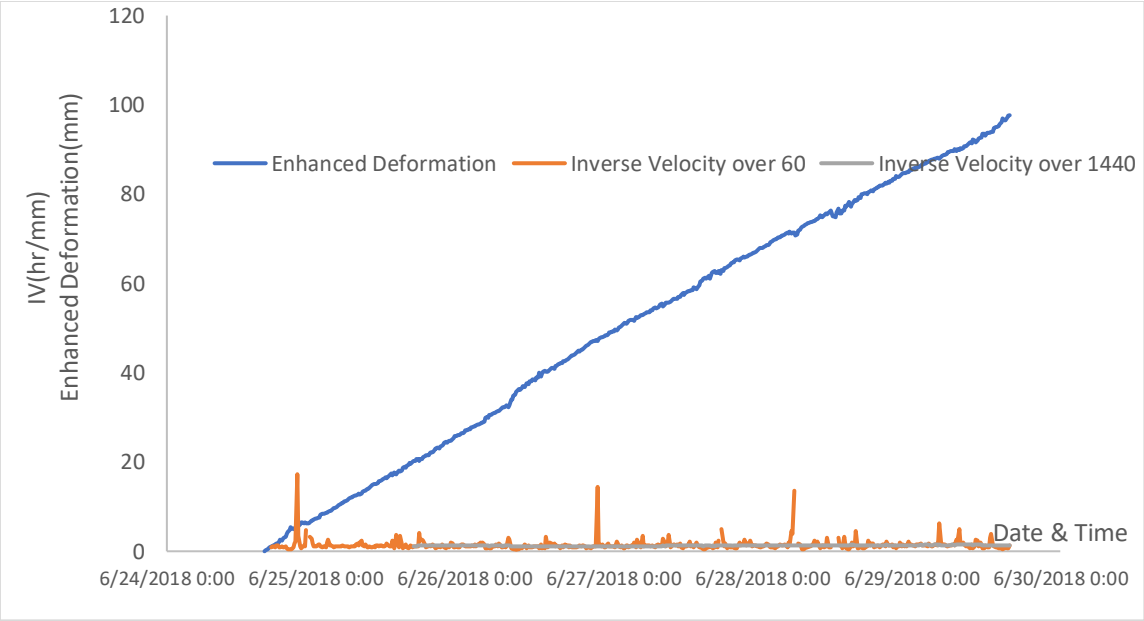

Figure 3. 2: Plot of enhanced deformation and inverse velocity over 60 and 1440 min with respect to time (date & time)

The figure 3.2 illustrates increasing Enhanced Deformation with time, indicating a decreasing trend in inverse velocity. However, when averaged over 60 and 1440 minutes, inverse velocity fluctuates over a four-and-a-half-day period. The trend line doesn't intersect the time axis conclusively. Despite the short monitoring period, slope face movement is not significant. Averaging data over intervals like 60 minutes, 480 minutes, and 1440 minutes simplifies and presents deformation info in a user-friendly manner. This aligns with practical needs, offering insights at varying temporal resolutions. Shorter intervals capture detailed changes, while averaged intervals provide a broader view. Simple Time Averaging in SSR data processing calculates mean values over specific intervals, aiding interpretation and pattern identification. It balances detailed data and clear, understandable deformation summaries. This enhances SSR data usability for monitoring and decision-making regarding slope stability.

Figure 3.3 presents the inverse velocity plot averaged over 60 minutes for the same wall as in Figure 3.1, but for a different selection area over seven days. The fluctuating inverse velocity forms a linear trend line. Manual inverse velocity calculation matched SSR-generated data. However, a trigger value couldn't be obtained due to the flat trend line.

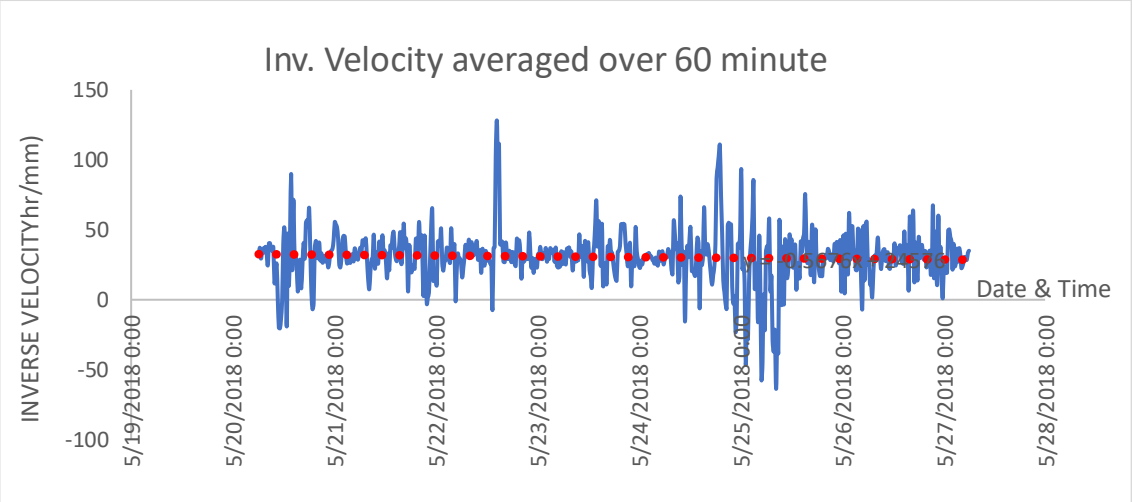

Figure 3. 3: Plot of inverse velocity with time averaged over 60 min period during 20-27 May 2018

In the next phase, the data for the period 24-06-2018 15:44 to 11-09-2018 13:02 was provided by the mine. Figure 3.4 shows the image of the scan area monitored by the SSR in this period.

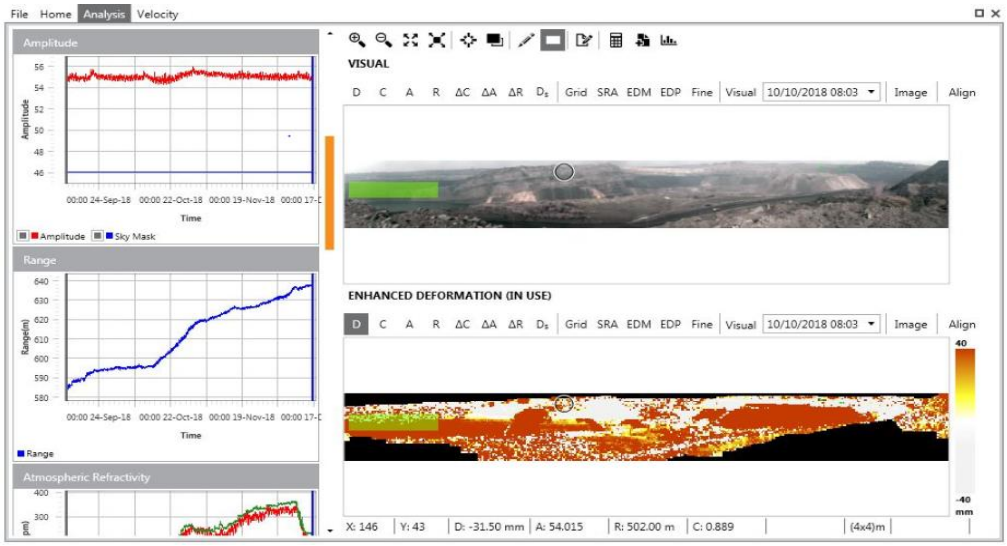

Figure 3. 4: SSR Viewer screen showing the image of the wall, the scanned area, the selection, and the heat map (16-07-2018 14:22 to 11-09-2018 17:05)

Figure 3.5(a) displays the enhanced deformation plot, illustrating no abrupt changes over time, suggesting a stable slope face with no significant deformation rates. Figures 3.5(b), 3.5(c), and 3.5(d) present inverse velocities and their trend lines obtained by averaging data over 60, 480, and 1440 minutes, respectively. The IV plots, while not conclusive in determining TLV, show trend lines not converging towards the time axis, indicating probable safety of the monitored face over the monitoring duration.

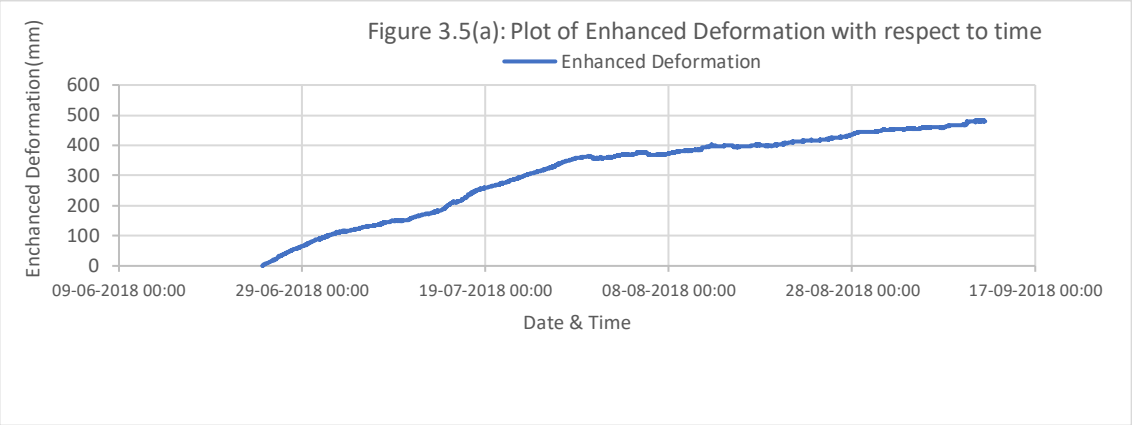
Figure 3.5(a): Plot of Enhanced Deformation with respect to time
Enhanced Deformation
Enchanced Deformation(mm)
600
500
400
300
200
100
0
09-06-2018 00:00
29-06-2018 00:00
19-07-2018 00:00
08-08-2018 00:00
28-08-2018 00:00
17-09-2018 00:00
Date & Time

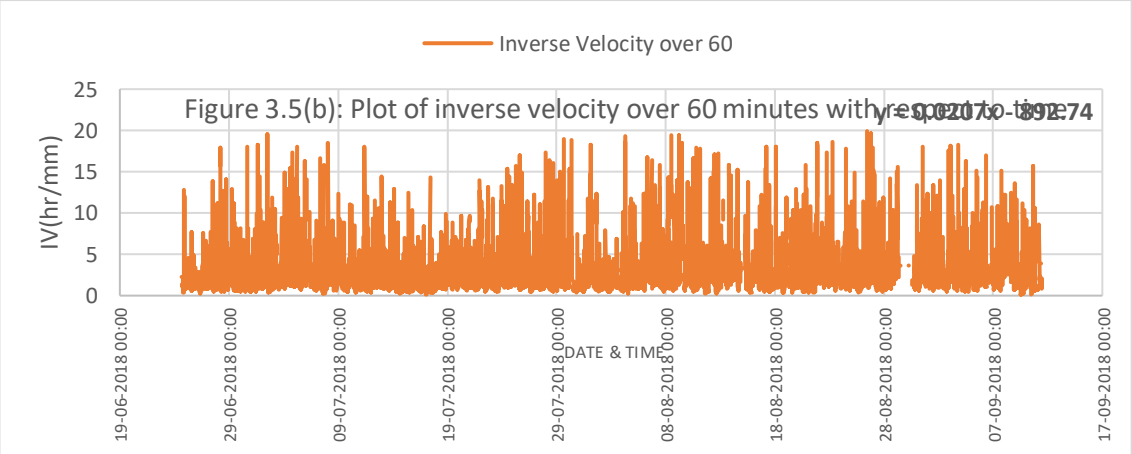
Inverse Velocity over 60
Figure 3.5(b): Plot of inverse velocity over 60 minutes with respect to time
IV(hr/mm)
25
20
15
10
5
0
19-06-2018 00:00
29-06-2018 00:00
09-07-2018 00:00
19-07-2018 00:00
29-07-2018 00:00
08-08-2018 00:00
18-08-2018 00:00
28-08-2018 00:00
07-09-2018 00:00
17-09-2018 00:00
DATE & TIME

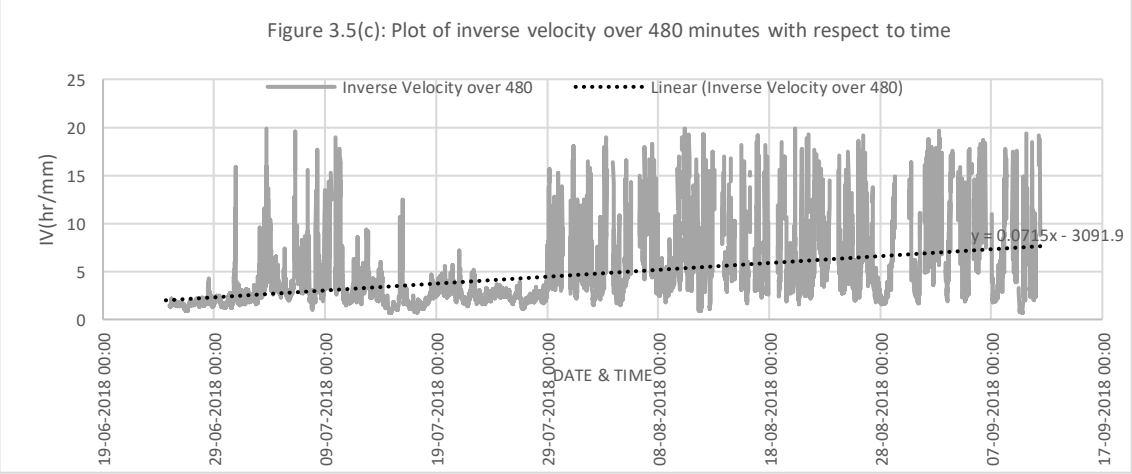
Figure 3.5(c): Plot of inverse velocity over 480 minutes with respect to time
Inverse Velocity over 480
Linear (Inverse Velocity over 480)
IV(hr/mm)
25
20
15
10
5
0
y = 0.0715x - 3091.9
19-06-2018 00:00
29-06-2018 00:00
09-07-2018 00:00
19-07-2018 00:00
29-07-2018 00:00
08-08-2018 00:00
18-08-2018 00:00
28-08-2018 00:00
07-09-2018 00:00
17-09-2018 00:00
DATE & TIME

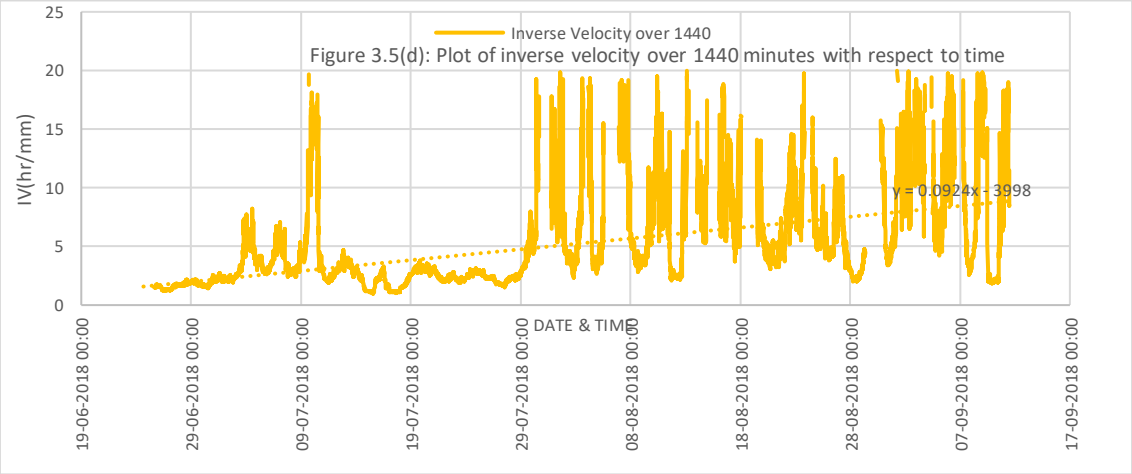

Figure 3. 5: Plot of Deformation & Inverse Velocity with respect to time

Furthermore, to achieve validate our predictions we take the next series of the data for the time period (11-09-2018 14:22 to 16-12-2018 17:05).

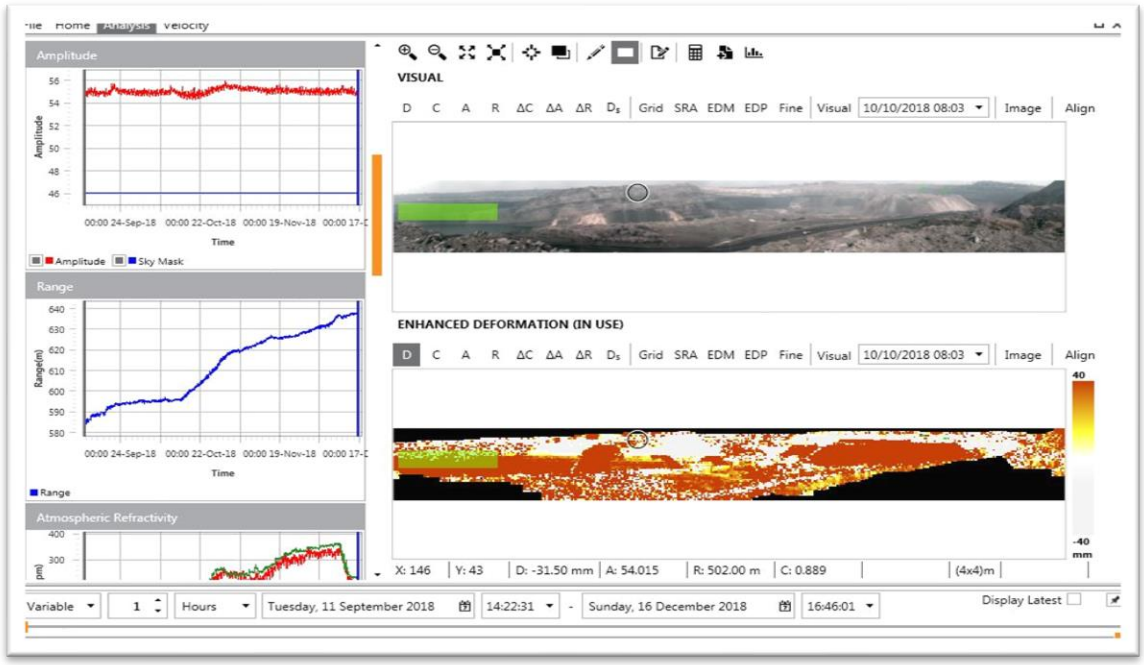

Figure 3. 6 : SSR Viewer screen showing the image of the wall, the scanned area, the selection, and the heat map (11-09-2018 14:22 to 16-12-2018 17:05)

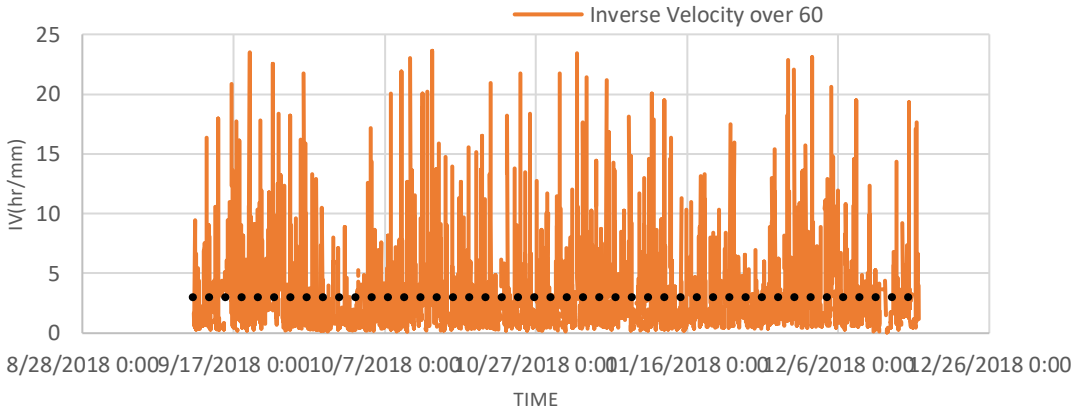

Figure 3.7(a): Plot of inverse velocity over 60 minutes with respect to time

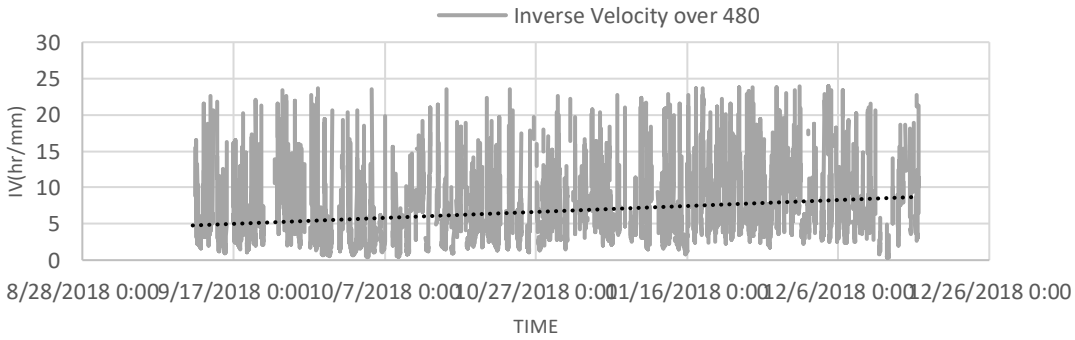

Figure 3.7(b): Plot of inverse velocity over 480 minute with respect to time

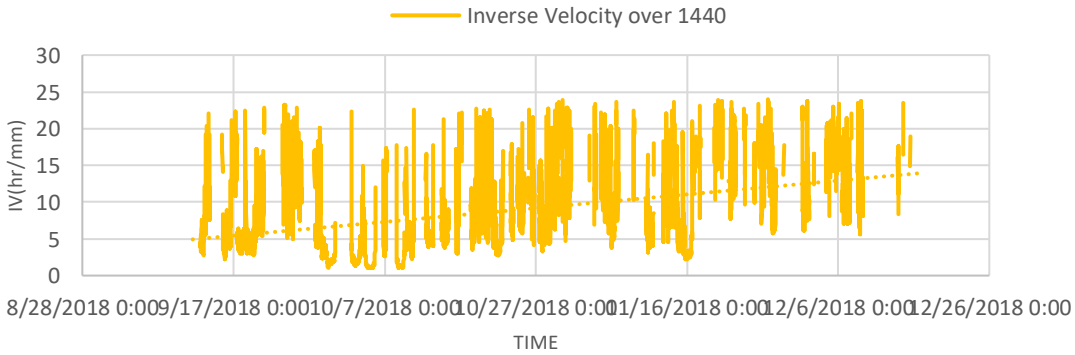

Figure 3.7(c): Plot of IV over 1440 minute with respect to time

Figure 3. 7 : Plot of Inverse Velocity vs Time

The inverse velocity trend lines, averaged over different durations (60, 480, and 1440 minutes), are presented in Figures 3.7(a-c). The trend lines exhibit a nearly flat trajectory for the 60-minute interval but display a positive gradient for the longer intervals, indicating decreasing deformation rates and a stable structure. However, it's noted that active mining during the monitoring period renders longer averaging undesirable for TLV determination.

Subsequent analyses, including Figure 3.8 and onwards, targeted the NCC Coal face, showing varying inverse velocity trends. For instance, Figure 3.9, focusing on 15-08-2017 to 16-08-2017, reveals a positive regression slope suggesting slope stability despite high cumulative deformation. However, different trend lines predicted varying failure times, showcasing the method's sensitivity to the choice of IV and trend lines.

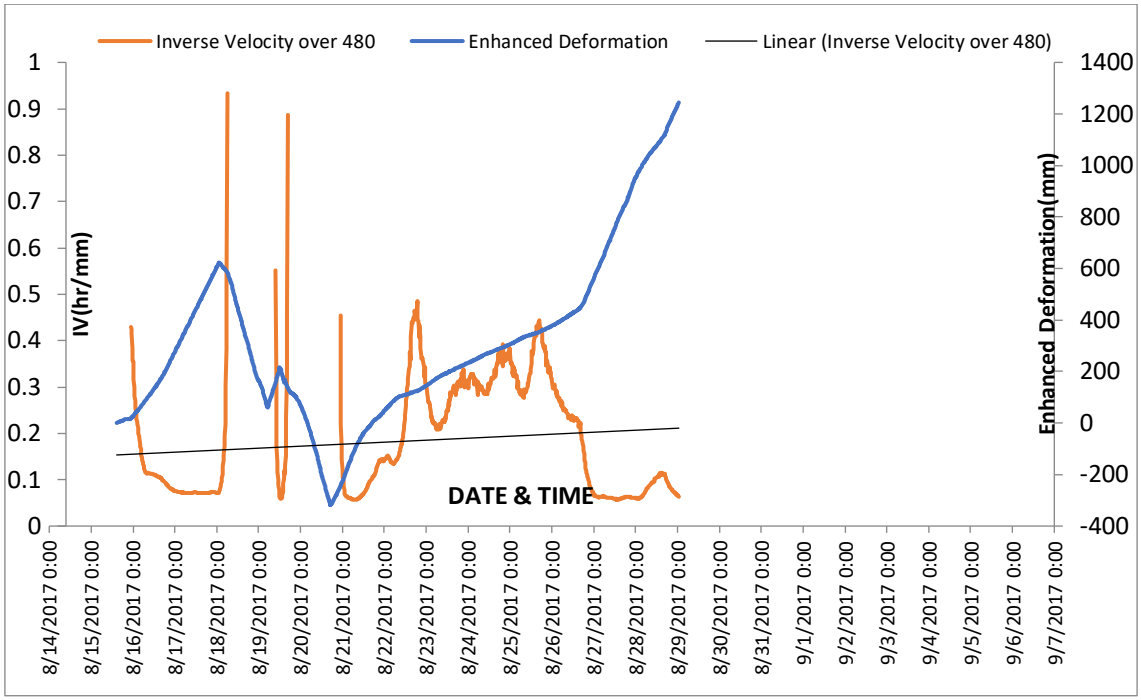

Figure 3. 8: Inverse velocity plot of ncc coal (58,34) for (15-08-2017-29-08-2017) averaged over 480 minutes

Notably, the plots capture the failure event on 16th August 2017, aligning closely with field observations. Consistent trend predictions are observed in Figures 3.8 to 3.13, with the IV over 60 minutes yielding the most accurate estimations. Specifically, Figure 3.12 provides the nearest prediction, pinpointing the failure onset at 11:03 am. A change in the selection area within the same wall alters the trends drastically, illustrated in Figure 3.14.

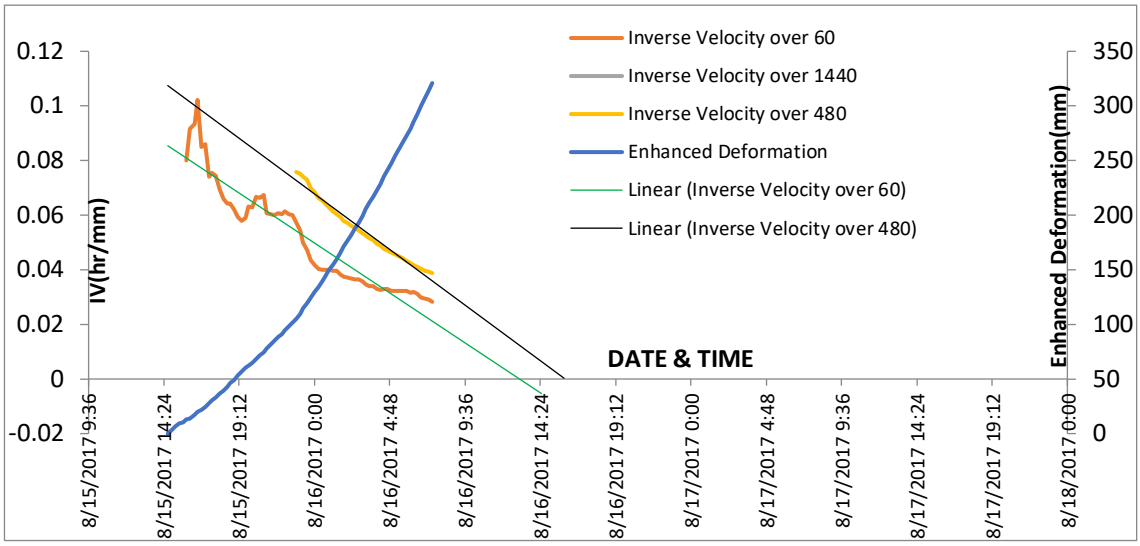

Figure 3. 9: Inverse velocity plot of ncc face for 15-08-2017-16-08-2017 averaged over 60,480, 1440 minute

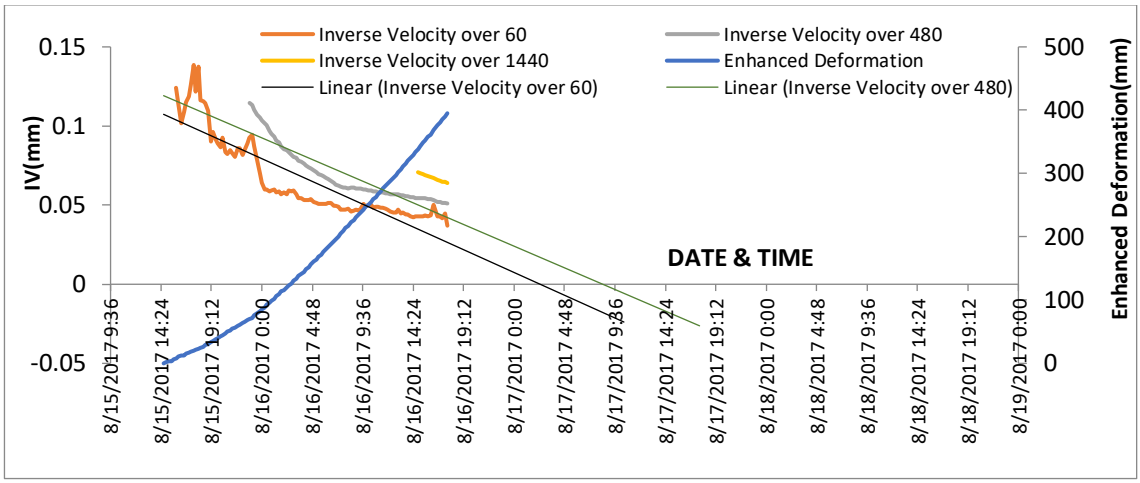

Figure 3. 10: Inverse velocity plot of ncc face for 15-08-2017 to 16-08-2017 over 60,480, 1440 minute

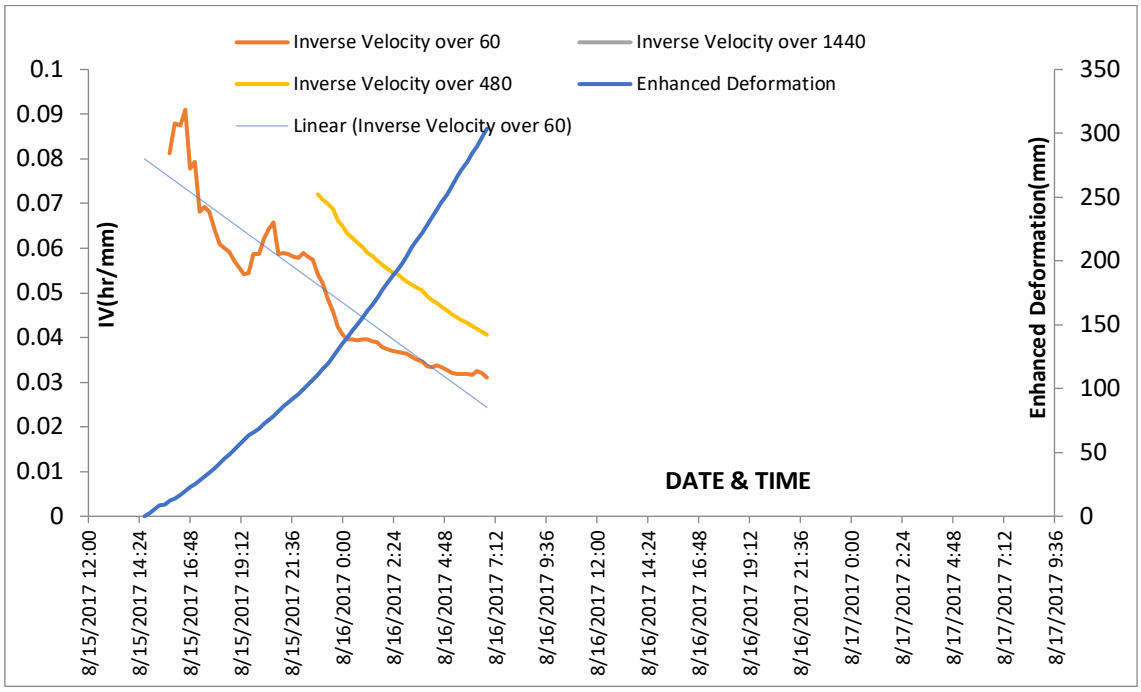

Figure 3. 11 : Plot of inverse velocity of ncc coal face pixel (61,37) for 15-08-2017-16-08-2017 averaged over 60,480, 1440 minute

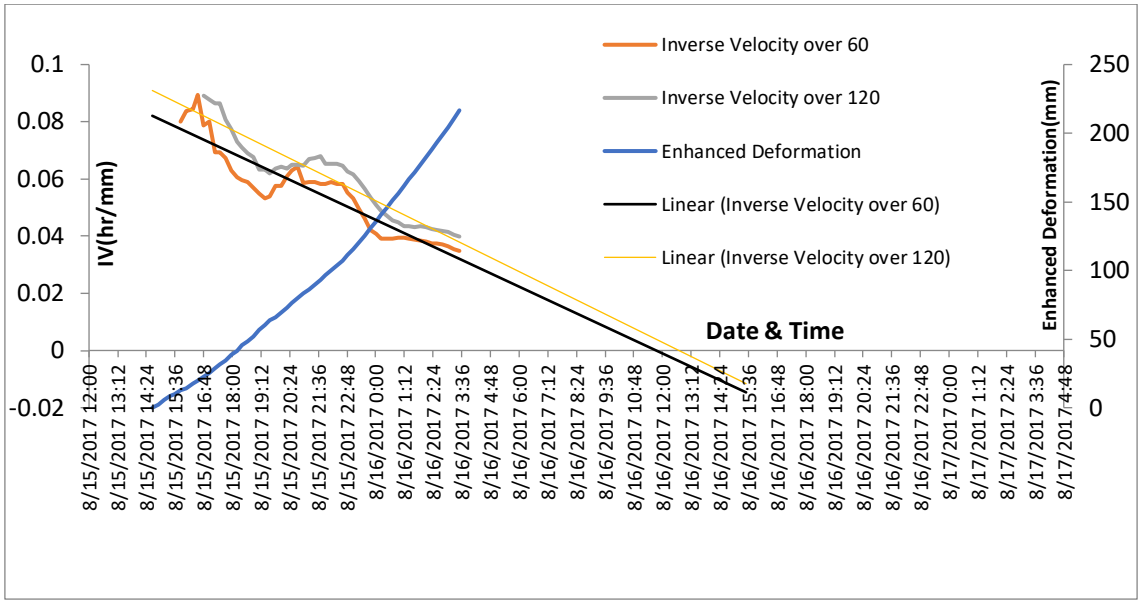

Figure 3. 12 : Inverse velocity over of ncc coal face for 15-08-2017-16-08-2017 averaged over 60 and 120 minute

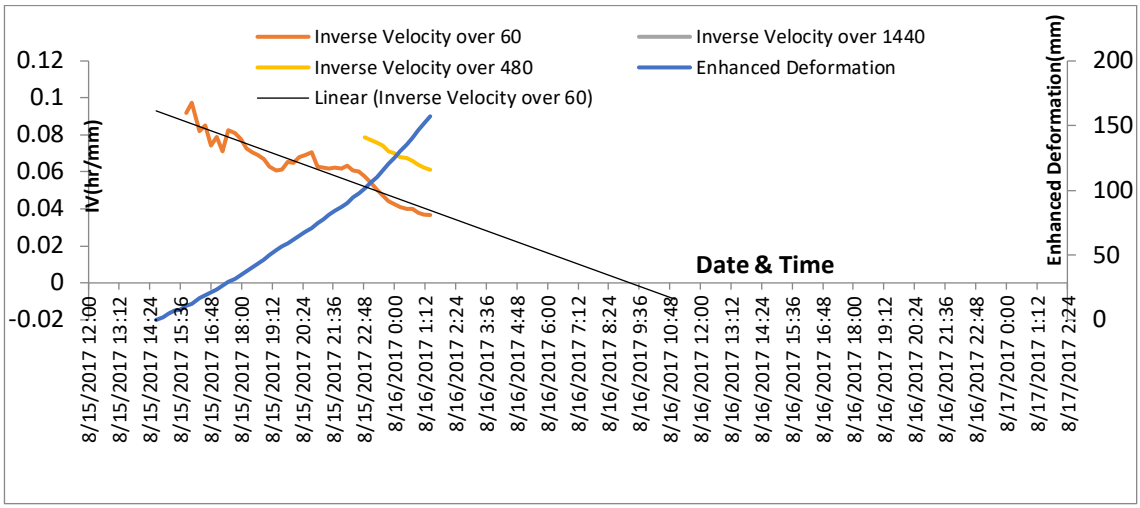

Figure 3. 13 : Inverse velocity plot of ncc face for 15-08-2017 to 16-08-2017 averaged over 60,480, 1440 minute

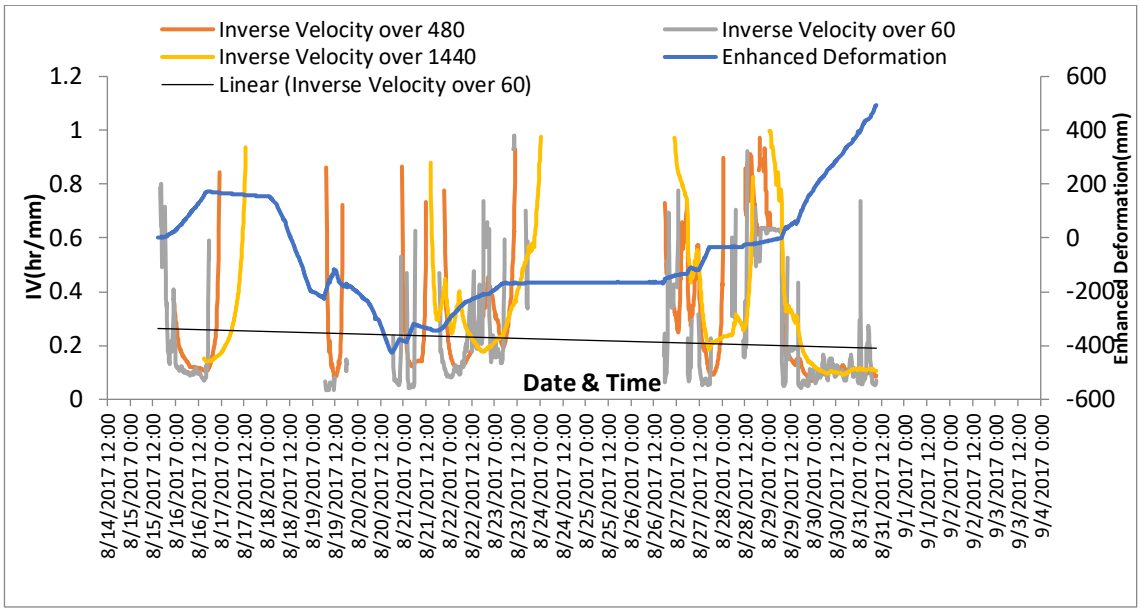

Figure 3. 14: Inverse velocity plot of selection area pixel (96,65) averaged over 60,480, and 1440 minute

In all the aforementioned cases, attempts were made to apply the inverse velocity method (IVM) using Microsoft Excel. However, determining the Threshold Limit Value (TLV) using this approach was unsuccessful. Furthermore, predicting the slope failure time through the IVM did not align with the actual failures, except in instances where SSR monitoring commenced just days before the actual failure event. The table below summarizes our analysis outcomes, prompting a re-evaluation of our methodology for

TLV determination and other slope-related thresholds, as well as for the prediction of slope failure.

Table 3. 1 : Results for determination of TLV using IVM in MS Excel

Figure No.	Location	Period	TLV
Figure 3.2	gpsp file	25-06-2018 to 29-06-2018	Not Conclusive (Probably Safe)
Figure 3.3	gpsp file	20-05-2018 to 27-05-2018	Not Conclusive (Probably Safe)
Figure 3.5(a,b,c,d)	NCC Wall Pixel (37,52)	16-07-2018 to 11-09-2018	Not Conclusive (Probably Safe)
Figure.3.7(a,b,c)	NCC Wall Pixel (146,43)	11-09-2018 to 16-12-2018	Not Conclusive (Probably Safe)
Figure 3.8	NCC Wall Pixel (58,34)	15-08-2017 to 29-08-2017	Not Conclusive (Probably Safe)
Figure 3.9	NCC Coal Face	15-08-2017 to 16-08-2017	Not Conclusive (Probably Unstable)
Figure 3.10	NCC Coal Face	15-08-2017 to 16-08-2017	Not Conclusive (Probably Unstable)
Figure 3.11	NCC Coal Face	15-08-2017 to 16-08-2017	Not Conclusive (Probably Unstable)
Figure 3.12	NCC Coal Face	15-08-2017 to 16-08-2017	Not Conclusive (Probably Unstable)
Figure 3.13	NCC Coal Face	15-08-2017 to 16-08-2017	Not Conclusive (Probably Unstable)
Figure 3.14	Pixel (96,65)	15-08-2017 to 31-08-2017	Not Conclusive (Probably Safe)

After obtaining the results outlined in Table 3.1, various other methods of data analysis were attempted to derive inverse velocities and velocities for the SECL mine slopes. However, these attempts yielded highly inconclusive results.

Subsequently, we conducted data analysis and devised an algorithm using MATLAB. MATLAB was chosen for the development of the Slope Failure Prediction Model for Surface Mines (SFPMSM). Over the years, MATLAB has evolved into a comprehensive programming language and development environment, supporting an extensive array of applications such as signal and image processing, machine learning, computational finance, control systems, and more. Besides its computational and programming

capabilities, MATLAB offers potent visualization tools, enabling the creation of 2D and 3D plots.

3.2 Development of Slope Failure Prediction Model for Surface Mines (SFPMSM)

A novel algorithm for determining an increasing stage from data on velocity (displacement rate) is proposed as a solution to slope failure prediction. Automatic operation has several benefits. The time analysis can be finished faster because the algorithm can be stopped if a single condition is not met. In a single dataset analysis, this option has a minor influence, but it becomes more and more critical in the context of several high-sampling rate systems. This strategy is designed to strike a compromise between the reliability of the results and the computational complexity. Including a tolerance component for conditions in a multi-criteria approach is possible. This could be used with any instrument that measures slope displacements conceptually. The proposed methodology relies on the following hypothesis:

- when a slope fails, its behaviour shifts from a secondary to a tertiary creep, and the displacement rate between two consecutive readings should increase.
- velocity that increases with time.
- the graph of displacement rate versus time is a concave growing curve.
- the regression of inverse velocity versus time is a straight line.

The algorithm is divided into 6 stages, and after getting the result as positive the onset-of -acceleration time will be identified, leading to the prediction of failure.

Stage 1

All the displacement values should be greater than or equal to zero.

$$d \geq 0$$

In Slope Stability Radar (SSR) monitoring, the deformation or displacement (d) is typically measured and analysed in a scalar form, considering the magnitude of displacement rather than vector displacement. The scalar deformation value represents the total displacement along the radar line of sight or the line connecting the radar antenna to a specific point on the slope. SSR systems are designed to measure the radar line-of-sight displacement, which is the component of displacement along the radar beam direction. This is the most relevant information for monitoring slope deformations in the context of SSR. The system captures the change in distance along the radar beam caused by the movement of the slope's surface.

Stage 2

This stage of the algorithm focuses at the rates of displacement (velocity). The inclusion of Stage 2 in the algorithm was implemented as a preliminary evaluation of displacement rates. Four consecutive positive velocities are required for progression through this phase. To get started, a dataset with four velocity values (i.e., five recordings of d) is required. If a slope is moving towards the monitoring device, the velocity is considered positive. Conversely, if the slope is moving away from the monitoring device, the velocity is considered negative. This step is crucial to getting relevant results from applying forecasting models, such as the IVM because a negative velocity would be meaningless in this context, effectively invalidating the forecasting analysis.

$$v = \frac{\Delta d}{\Delta t}$$

$$v > 0$$

$$v_i > 0$$

$$v_{i+1} > 0, v_{i+2} > 0, v_{i+3} > 0$$

$$v_i=(d_i-d_{i-1})/(t_i-t_{i-1})$$

where, v_i is the velocity at i, d_i & t_i are displacement and time (date, expressed as a number) corresponding to i.

Hence if, $v_i, v_{i+1}, v_{i+2}, v_{i+3}, v_{i+4} > 0$; then the algorithm goes to the next stage; otherwise, will return to stage 1 again.

Stage 3

If stage 2 produces a positive output, the next stage checks the difference between two consecutive readings to see if the velocity increases using data. The condition is deemed satisfied if at least three of the dataset's four successive velocity values meet the criteria ($\mathbf{v_i < v_{i+1}}$, for 75% of the data). The primary purpose of this tolerance margin is to avoid mistakes resulting from anomalies (outliers or noise) in monitoring data. In reality, an excessively severe condition considering a complete validation condition of the all the displacement or velocity values in the dataset to give a positive outcome may perceive even one negative output at the stage as a real slowing of the movement; however, its length may be minor compared to the overall trend of the slope movement, this would end the whole algorithm at this stage. This tolerance margin allows the analysis to go forward even if an anomalous value is recorded.

Stage 4

This stage assumes that velocities will behave non-linearly throughout the acceleration periods. Following this hypothesis, we try a curve-fitting approach to the given displacement rate vs. time data to find and check the slope deformation rate behaviour. In the literature, we have encountered cases that use power law for velocity data to properly define the phases of the creep in the evolution of potentially unstable slopes. Nevertheless, while this approach was calibrated and tested for many data sets of multiple

random dataset windows, the power law function results had a poor correlation with the original data. The problem with the power law function is that it only gave reliable results when applied to later stages of the slope movements and not to our whole algorithm designed to interpolate a general trend. To circumvent the difficulty, we tried a curve-fitting approach employing a parabolic function to detect trends (upward or downward) by examining the direction of velocity vs time curve concavity. Figure 3.15 exhibits four distinct examples resulting from the data analysis, illustrating a comparison between two separate approaches for curve fitting i.e., the parabolic and the power law.

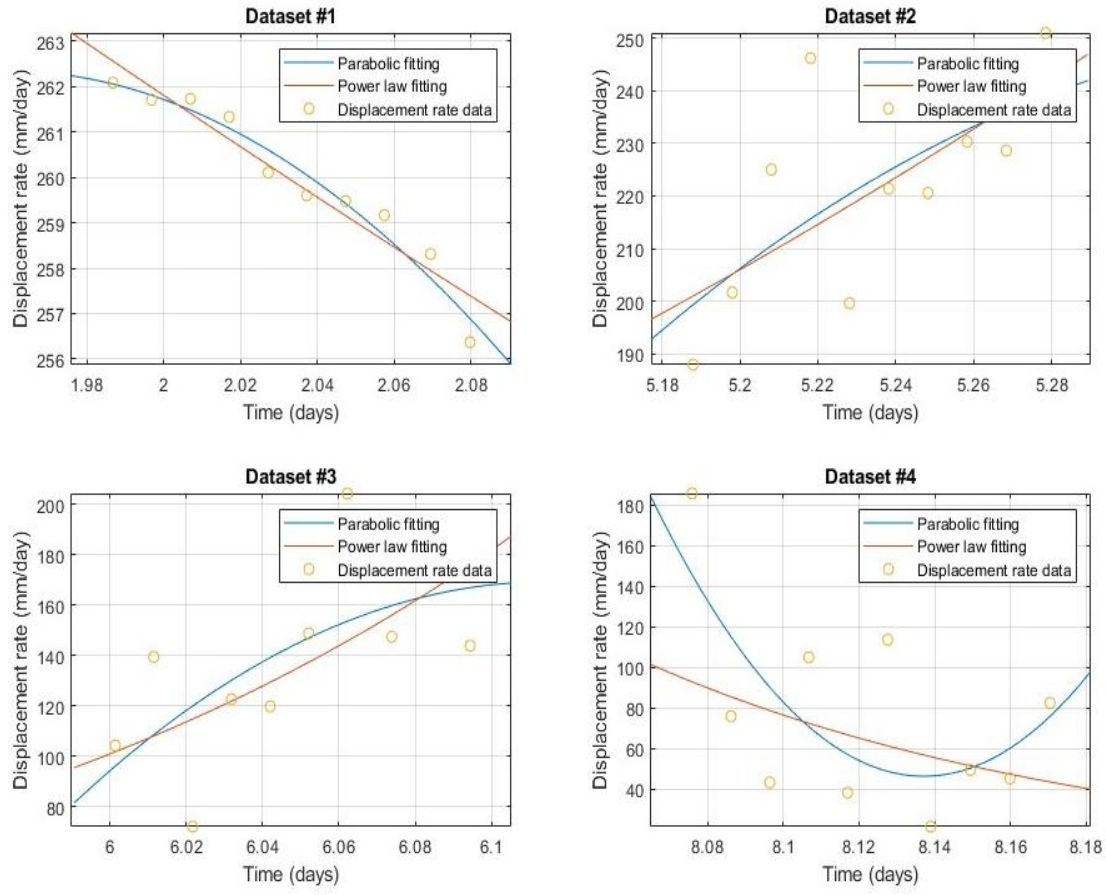

Figure 3. 15: Trend analysis using MATLAB

The general equation of a parabola is $y=ax^2+bx+c$

Evaluating the' a' coefficient of the interpolating curve is the primary goal of stage 4, which provides information on the curve's concavity. In this algorithm stage, the velocity

data is interpolated using a parabolic fit to determine the concavity direction represented by the parameter 'a'.

An accelerating phase (a>0) displays the concavity upwards, whereas a de-accelerating phase has a<0 and the orientation of the concavity are reversed. In the proposed method, a positive value of ‘a’ is monitored to determine acceleration. If a>0 is valid for at least $3/4^{th}$ of the data, stage 4 is completed, and the analysis can go on to the next stage.

Stage 5

In this stage, the change in the 'a' coefficient between two measurements is checked for the significant concavity orientation in the monitoring data curve (i.e., the acceleration decreases or increases if there is a downward or upward orientation). No change in the value of 'a' suggests the curve is becoming more linear, which shows a decrease in slope movements. Stage 5 is initiated if three of four data points are correct (75 percent of the dataset). If this condition returns true, in this case, an accelerating phase may be underway, and the ‘i’ value of time is interpreted as the commencement of acceleration of the measured slope.

A parametric analysis had to be carried out on several datasets from the literature and field data collected to validate the proposed methodology. This schematic diagram (Figure 3.16) outlines the parabolic fitting process and the subsequent analysis of parameter 'a' to determine concavity orientation. The conditions a>0, a=0 and a<0 are specified, indicating different phases based on the concavity of the interpolating curve.

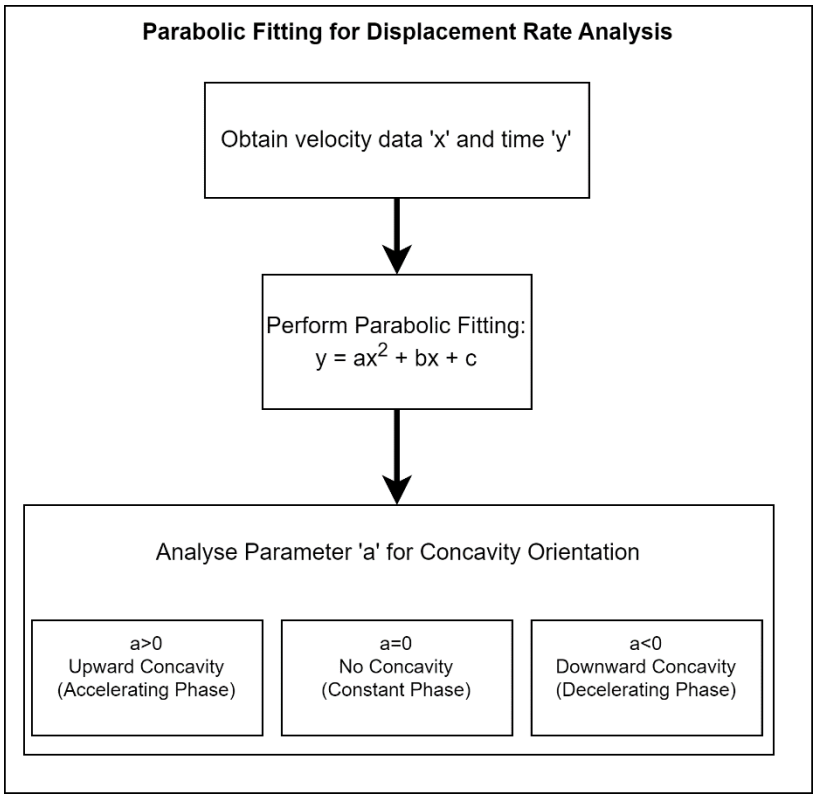

Figure 3. 16: Schematic diagram showing the concavity direction with respect to ‘a’

Stage 6

If the algorithm returns a TRUE for stage 5, the onset of failure time is identified. This time can be used as an input for the failure prediction. The time of onset will be set as the “zero” time(t=0) on the time axis of the Inverse Velocity vs Time graph. Where the graph cuts the time axis will be the predicted failure time.

The reason for the limit of 75% data in this stage of the algorithm can be understood by the parametric analysis conducted. This analysis focused on the number of monitoring data to consider in the onset of failure or onset of acceleration identification process. Moreover, the study included different rate limit values (i.e., the percentage of positive data points required to fulfil a specific requirements of a stage) to highlight their influence on the acceleration phase assessment, as well as the generation of possible false positives. Comparisons were made between the reference dataset of d = 4 monitoring data, featuring

a 3/4 limit (i.e., 75%), with a 5-point dataset characterised by two different rates, namely 3/5 (60%) and 4/5 (80%). The same reference case compared to a 6-point dataset with a rate of 4/6 (67%) and 5/6 (83%).

The presented findings are based on an examination of historical data, utilizing 10 monitoring data points for fitting a parabolic model. Analysis of these outcomes yields the following observations:

In terms of onset time estimation, all setups yielded similar results, except for the d = 6, 4/6 model, which predicted it a day earlier. Increasing the number of data points resulted in a delay in meeting Stage 5 conditions, postponing onset identification. This delay is a notable limitation, especially for a methodology aiming at timely early warning assessments. Higher percentage limits compared to the reference value did not notably enhance the prevention of false positives. An exception is the 83% rate in the d = 6 configuration, although it significantly delayed the estimation of the onset. Conversely, values below 75% increased false positives for both d = 5 and d = 6 configurations.

A parametric analysis was conducted on the number of monitoring data points used in the parabolic model fitting, derived from two datasets, employing a d = 4, 3/4 configuration. Examination of the results underscores the influence of the "n" parameter on false positives occurrence. Specifically, "n" values of 10 exhibited a higher number of data points fulfilling Stage 5 conditions, resulting in false positives before the actual acceleration onset. Datasets with fewer data points showed reduced reliability in assessing the critical acceleration phase. Analyses conducted with datasets ranging from 10 to 12 points consistently met Stage 5 conditions after onset identification. On the other hand, configurations with "n" = 8 and "n" = 9 failed to provide a dependable assessment of the acceleration onset, as the analyses did not reach the algorithm's higher level during the critical acceleration phase, leading to an imprecise onset definition.

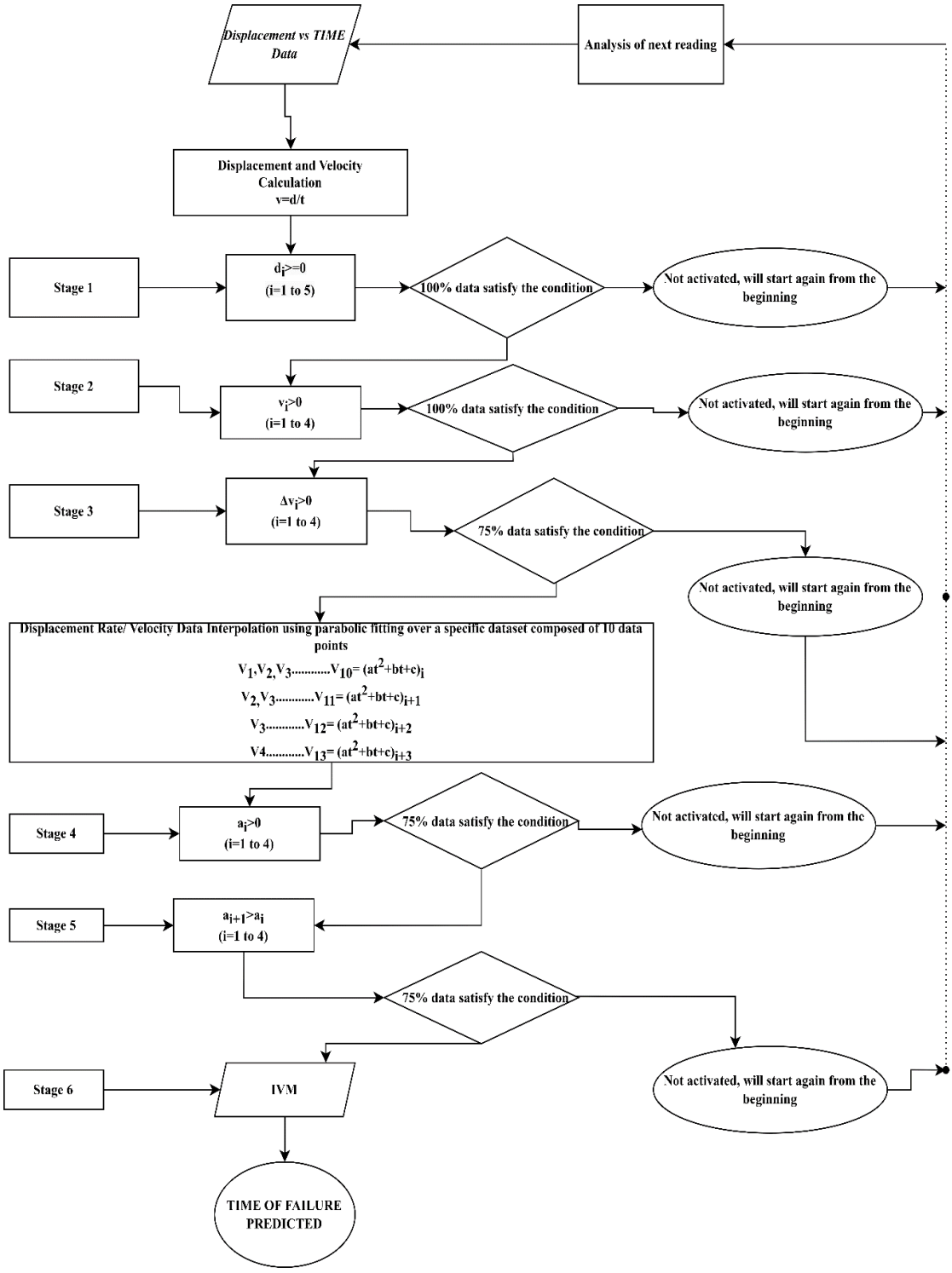

Figure 3. 17 : Algorithm Flow-Chart for finding the onset of acceleration and prediction of failure of a surface mine slope

This algorithm for finding the onset of acceleration and prediction of failure of a surface mine slope can used to predict the onset of acceleration only without going to the Stage 6 where the IVM Stages acts. The output by using this algorithm till stage 5 gives us thresholds of velocity and displacement as well. After the onset of acceleration/ onset of failure time is detected using the algorithm, the IVM will predict the time of failure.

The key differentiator between the Slope Failure Prediction Model for Surface Mines (SFPMSM), devised in this study, and the IVM lies in their fundamental approach to predicting slope failure. The IVM relies only on the calculation of inverse velocity. However, it's crucial to note that the IVM is effective in predicting failure only after the initiation of acceleration within the slope, a pivotal turning point in its deformation trajectory. In contrast, the developed model adopts a more comprehensive approach. It not only considers the inverse velocity but also accounts for various other critical parameters associated with slope movements. This encompasses a thorough analysis of displacement patterns, assessment of critical thresholds linked to slope movements, and the ability to set up alarms based on these thresholds. The SFPMSM excels in evaluating diverse aspects of slope behaviour and deformation patterns, offering a broader perspective. Furthermore, it integrates a multi-stage methodology, enabling real-time application by automatically defining the time of activation, particularly at the OOA/OOF. This ensures that the prediction process is dynamic and responsive, adapting to changing slope conditions. By using a comprehensive set of analytical tools, the model provides a highly accurate and timely prediction of slope failure, significantly enhancing the reliability and effectiveness of slope monitoring and prediction in mines.